HHS Public Access

Author manuscript

Nat Rev Cancer. Author manuscript; available in PMC 2019 February 12.

Published in final edited form as:

Nat Rev Cancer. 2017 December ; 17(12): 738–750. doi:10.1038/nrc.2017.93.

Transport of drugs from blood vessels to tumour tissue

Mark W. Dewhirst[1] and **Timothy W. Secomb**[2]

[1]Department of Radiation Oncology, Duke University Medical Center, Durham, North Carolina 27710, USA.

[2]Department of Physiology, University of Arizona, Tucson, Arizona 85724, USA.

Abstract

The effectiveness of anticancer drugs in treating a solid tumour is dependent on delivery of the drug to virtually all cancer cells in the tumour. The distribution of drug in tumour tissue depends on the plasma pharmacokinetics, the structure and function of the tumour vasculature and the transport properties of the drug as it moves through microvessel walls and in the extravascular tissue. The aim of this Review is to provide a broad, balanced perspective on the current understanding of drug transport to tumour cells and on the progress in developing methods to enhance drug delivery. First, the fundamental processes of solute transport in blood and tissue by convection and diffusion are reviewed, including the dependence of penetration distance from vessels into tissue on solute binding or uptake in tissue. The effects of the abnormal characteristics of tumour vasculature and extravascular tissue on these transport properties are then discussed. Finally, methods for overcoming limitations in drug transport and thereby achieving improved therapeutic results are surveyed.

In order for cancer chemotherapy to have lasting effects, drugs must be applied to a large fraction (close to 100%) of cancerous cells. Many factors influence the effectiveness of chemotherapeutic treatment, including the size, charge, lipid solubility and acid-base characteristics of drugs, the dosing level and schedule, the pharmacokinetics of drug residence in the circulation, the pharmacodynamics of cell killing in response to drug exposure, the presence of cellular drug resistance pumps and the use of radiation, surgery or other treatments in combination with chemotherapy. All these factors have been intensively considered in studies of cancer chemotherapy[1]. Herein, the term ‘drug’ is used in a broad sense to include molecules with low relative molecular mass (M_r) and those with high M_r and nanoparticles.

Correspondence to M.W.D. mark.dewhirst@duke.edu.

Author contributions

M.W.D. accepted the commission to prepare this Review and prepared the outline in collaboration with T.W.S. M.W.D. researched data in collaboration with T.W.S. M.W.D and T.W.S. contributed equally to writing and revising the text.

Competing interests statement

T.W.S. has no conflicts of interest. M.W.D. was involved in the development of the thermally sensitive liposome described in this paper and has stock in Celsion Corporation, the company that licensed the drug. M.W.D. is also a consultant for Siva Therapeutics and Kaio Therapy and a member of the Scientific Advisory Board of Innovate Biopharmaceuticals.

Publisher’s note

Springer Nature remains neutral with regard to jurisdictional claims in published maps and institutional affiliations.

For chemotherapy of solid tumours, a drug delivered via the bloodstream must be capable of traversing walls of blood vessels and the surrounding tissue to reach tumour cells that are located at varying distances from the nearest vessel (FIG. 1). These transport processes depend not only on the properties of the drug but also on physiological characteristics, including the structure and flow distribution in the system of microvessels supplying the tumour, and on the properties of extravascular tissue components, including the extracellular matrix (ECM), normal cells, tumour cells and interstitial spaces (TABLE 1). Therefore, treatment efficacy is strongly dependent on microvascular structure and function and on drug transport properties in tissue. However, these characteristics have generally received little attention in the design of drugs and treatments for solid tumours.

Aspects of drug transport to solid tumours have been considered previously in several reviews. Swabb *et al.*x[2] considered the relative importance of diffusive and convective transport of drugs in tissue. Importantly, Jain and colleagues[3–7] emphasized the importance of transport characteristics for all types of drugs, from small molecules to antibodies and nanoparticles. Theoretical approaches for analysing drug delivery were reviewed by El-Kareh and Secomb[8]. Ribatti et al.[9] reviewed studies on the structure of tumour blood vessels. The hyperpermeability of tumour microvasculature to macromolecules and nanoparticles, known as the enhanced permeability and retention (EPR) effect, was reviewed by Maeda *et al.*[10]. Minchinton and Tannock[11] reviewed methods for assessing and modifying the ability of drugs to penetrate solid tumours.

The objective of this Review is to define the main factors influencing the transport of drugs from blood to tumour cells, to outline the physical principles that underlie the dependence of transport on drug characteristics and to present an overview of current strategies to enhance treatment efficacy by improving drug delivery. Unique aspects of this Review include a quantitative analysis of the factors governing drug penetration distance into tissue and a systematic review of the improvements in drug delivery that have been achieved by various methods. Increased awareness and consideration of drug transport properties will, we hope, contribute to the development of more effective drugs and treatment strategies.

Fundamentals of mass transport

Physical basis of convection and diffusion.

The basic mechanisms of biological mass transport are molecular diffusion, in which random molecular movements lead to net transport of solutes or particles down the gradient in concentration (or, more precisely, down the gradient in thermodynamic potential) and convection, in which a solute or particle is carried by a moving fluid. The solute flux resulting from molecular diffusion is proportional to the gradient in concentration. Therefore, diffusion is most effective over very short distances. Conversely, the range of convective transport is limited only by the distance over which the convective fluid is flowing. Active and carrier-mediated transport processes occurring across cell membranes and within cells may also be important, for instance, in cellular uptake of drugs, but are not considered in detail here. In a region where a fluid (for example, blood or interstitial fluid) is flowing, diffusive and convective transport can occur simultaneously. It is helpful to define a parameter that indicates the relative magnitudes of convective and diffusive solute fluxes: the

Péclet number *(Pe)* (BOX 1). Convective transport is dominant at high *Pe* (much greater than one), and diffusive transport is dominant at low *Pe* (much less than one).

Within blood microvessels, a typical velocity is 1 mm s^{-1} and a typical length scale (vessel length) is 1 mm. For a small solute with a diffusivity of 10^{-5}cm2 s^{-1}, the resulting *Pe*= 1,000, and so transport in the flow direction is dominated by convection. This is also the case for larger solutes with lower diffusivities. However, transport of small solutes in the radial direction may be dependent on diffusion, because the flow velocity in the radial direction is smaller and the relevant length scale, the vessel diameter, is of the order of 10 μm in microvessels.

In extravascular tissue, the typical distance for transport from vessels to tissue is of the order of 100 μm. A typical tissue fluid flow velocity[12] is 1 μm s^{-1}, but it may be smaller than this and may cease in regions of tumour tissue because of the lack of lymphatic drainage[13]. For a small solute with a diffusivity of $10^{-5}cm^2s^{-1}$ and an interstitial velocity of 1 μm s^{-1}, *Pe* = 0.1, and thus diffusive transport is dominant. However, for a high-M_r drug or a liposome or nanoparticle, *Pe* may be large. For example, a diffusivity of $10^{-7}cm^2$ s^{-1} gives *Pe*= 10 for the same values of the other parameters. Therefore, the relative contributions of convective and diffusive transport in tissue may vary widely depending on the solute diffusivity and the local interstitial fluid velocity.

Transport across vessel walls.

The walls of microvessels present a barrier to solute transport that depends on the type of solute and on the structural characteristics of the vessel[3,14]. The layer of endothelial cells forms the main transport barrier. Small lipophilic solutes (including nonpolar molecules such as oxygen) can easily diffuse through these cells because they are highly soluble in cell membranes. Other solutes (that are hydrophilic and/or large) must pass through gaps in the endothelial barrier. In continuous capillaries, narrow clefts between endothelial cells are the main pathway for small hydrophilic solutes. In the brain, the permeability of capillaries to small hydrophilic solutes is particularly low[15]. Conversely, microvessels in inflamed normal tissues and in tumours typically show increased numbers of larger gaps between endothelial cells, which allow higher permeability to solutes of all sizes, including large solutes[10]. The hydraulic conductivity of vessels is generally higher in tumours than in normal tissues, with important consequences, as discussed below.

Penetration of solutes into tissue.

The distance that a solute can be transported into tissue by diffusion or convection is limited by the rate at which it is taken up by tissue components. In general, the penetration distance depends on the ratio of the strength of the transport mechanism to the net rate of solute uptake. A simplified analysis yielding quantitative estimates of penetration distance is presented in BOX 2. Several different cases arise, depending on the type of transport (convection or diffusion) and the kinetics of solute uptake. For example, the low-M_r drug doxorubicin has a relatively high net cellular uptake rate due to its sequestration within intracellular compartments, which limits the predicted penetration distance to about 85 μm (BOX 2). Experimental observations[16] showed comparable results, with the concentration of

doxorubicin decreasing to half its perivascular concentration at a distance of about 40 to 50 μm. Tissue oxygenation strongly affects tumour responses to radiation and chemotherapies[17,18]. The maximum diffusion distance of oxygen from blood vessels is about 100 μm (BOX 2). Tumour tissue becomes hypoxic if a blood vessel containing oxygenated blood is not present within such a distance. Thomlinson and Gray[19] examined tumour cords in lung cancers and found necrosis at distances of 150 μm or more from the tumour periphery, which was supplied by blood vessels. They deduced the presence of viable hypoxic cells in tumours, as confirmed by subsequent investigators[20]. The difficulty of treating hypoxic cells has stimulated the development of drugs, such as tirapazamine, that are converted from an inactive to an active form when they enter hypoxic regions[18,21]. A computational simulation of the spatial distribution of both oxygen and drugs in the tissue surrounding a three-dimensional tumour microvascular network yielded predictions for the antitumour activity of tirapazamine analogues combined with radiation that agreed well with experimental observations[22].

The penetration distance of a solute into tissue can also be limited by the rate of diffusive spread with time. The typical time taken to penetrate a distance L is given by $t_D = L^2/D$ where D is the diffusivity. For a typical maximum diffusion distance from blood $L \approx 100$ μm, t_D ranges from a few seconds for small solutes to tens of minutes for high-M_r agents. In most cases, the residence time of drugs in the plasma is longer than this, and so the diffusion time is not limiting. However, penetration may be limited by this effect for high-M_r agents if the plasma residence time is unusually short or if the diffusion distance is very long. Effects on drug delivery over heterogeneous distances between areas in the tissue and the nearest vessel have been analysed by Baish *et al.*[23].

Drug transport in the circulation

Distribution in the vasculature.

Most anticancer drugs reach tumour sites by convection in the blood. Blood typically takes less than one minute to traverse the entire circulatory system, and the heterogeneous branching structure of the circulation ensures that solutes are well mixed in the blood within a few minutes, with the exception of substances with high first-pass metabolism. For a given dose, the site or route of delivery therefore has relatively little effect on the ultimate distribution, and all organs including the heart and lungs are exposed to the drugs (FIG. 1). For example, even in the case of a drug being delivered intraperitoneally, drug delivery is enhanced by diffusion directly from the intraperitoneal space only within a region of width about 0.5 mm[24]. Beyond that distance, delivery from the microvasculature is predominant.

Effects of tumour microvascular structure and function.

Structural abnormalities of tumour vasculature relative to the host tissue are commonly observed[9]. Tumour endothelial cells proliferate faster but form less tight junctions than endothelial cells in normal tissue[9]. Production of vascular endothelial growth factor (VEGF) by tumour cells is an important factor causing leaky endothelial cell junctions and hyperpermeability[25,26]. Tumour blood vessels often show increased tortuosity. Tortuosity is a feature of abnormal vessel growth; it tends to increase flow resistance[27]. Conditions of

hypoxia and acidosis decrease red blood cell fluidity and increase viscous flow resistance[28–30]. Patterns of arterial supply vessels are irregular[31], and oxygen levels may drop substantially in the arterial vessels, contributing to tissue hypoxia[32]. The typical hierarchical structure of microcirculation in normal tissue is often lacking in solid tumours. In normal tissues, vessel diameter decreases as branch order increases, but this is not consistently true in tumours[33]. In normal tissues, flow velocity scales approximately in proportion to diameter[34], but in tumours, there is virtually no relationship between vessel diameter and flow velocity[35]. Aberrant microvascular network structure can cause inefficient delivery of oxygen and drugs, even when the overall vascular density is high[36–38].

Perivascular oxygen levels may show little or no correlation with blood flow in tumours, and hypoxia may be present in the areas adjacent to flowing vessels[39,40]. Red blood cell fluxes in tumour microvessels show large, irregular fluctuations over periods of 10–20 minutes, with corresponding fluctuations in local oxygen levels and periods of transient hypoxia in some regions[41]. This phenomenon, referred to as intermittent or cycling hypoxia, can induce physiological responses that influence tumour angiogenesis and responses to chemotherapy and radiation[17,42].

The presence of vascular shunts reduces the efficiency of mass transport to tissue, because they divert blood flow to other parts of the tissue. In some tumours, arteriovenous shunt vessels have been identified[43–47]. Even in the absence of identifiable anatomical shunts, the tumour microcirculation may be subject to ‘functional shunting’ (REF. 48)(FIG. 2). A functional shunt can occur when a short flow pathway is connected in parallel with a long flow pathway. The rate of blood flow in a vessel is sensitively dependent on the vessel diameter, and a relatively small increase in diameter of a vessel forming a short flow pathway can cause flow to be diverted from the longer pathway to the short pathway. In microcirculatory networks, flow pathway lengths are highly heterogeneous. In normal tissues, efficient flow distribution is achieved by a set of structural adaptation mechanisms. Vessel internal diameter and wall thickness increase or decrease in response to changes in vessel wall shear stress, intravascular pressure and levels of oxygen and other metabolites[49]. Moreover, propagation upstream of signals along vessel walls is required to ensure adequate blood flow along the longer flow pathways. These signals, known as conducted responses, depend on exchange of ionic currents between endothelial cells and smooth muscle cells via gap junctions[50]. Pries *et al.*[48] hypothesized that conducted responses are compromised because of poor coupling between endothelial cells in tumour vessels and that this leads to functional shunting and impaired delivery of oxygen and drugs to tumour tissue. Direct experimental verification of this hypothesis remains to be obtained.

Drug transport into tissues

Transport through microvessel walls.

As a result of abnormal junctions between endothelial cells, the endothelial barrier of tumour microvessels is moderately leaky[9]. The permeability of tumour vessel walls to albumin[51] (M_r 69,000, Stokes-Einstein radius 3.5 nm) is around 10^{-7}cms^{-1}, approximately 10× higher than that of continuous normal capillaries[14]. The increased number of large pores in tumour microvessels allows passage of nanoparticles such as liposomes with a diameter of

~100 nm, for which the permeability is ~2× 10^{-8} cms^{-1} (REF. 52). These characteristics of macromolecule and nanoparticle transport have been termed the EPR effect[10]. In addition, the collagen content of the vessel wall affects the permeability to nanoparticles[53]. Heterogeneity in endothelial cell pore distribution and size can lead to spatial variations in nanoparticle delivery to the extravascular space, and the penetration distance of nanoparticles into tissue is typically very short[54]. If the nanoparticle releases a low-M_r drug into the interstitial space, the drug may spread by diffusion and achieve good spatial distribution in the tissue. The magnitude of the EPR effect is highly variable in human tumours[55,56]. For example, in women with metastatic breast cancer, the variability in EPR as assessed by positron emission tomography (PET) tracer-labelled nanoparticles was associated with progression-free survival after treatment with the same nanoparticles loaded with chemotherapy [57]. One of the challenges in studying the EPR effect in preclinical models is that they often exhibit a highly permeable phenotype, typified by very high VEGF production. It has been recommended that mouse models that are more likely to exhibit EPR characteristics of human tumours, such as patient-derived xenografts (PDXs) and genetically engineered mouse models (GEMMs), should be implemented. Additionally, it is important to evaluate drug delivery in both orthotopic and metastatic tumour sites[58].

Fluid filtration through microvessel walls is the primary driver of flow in the interstitial space, which can cause convective transport of solutes, as mentioned above. The rate of filtration depends on the hydraulic conductivity L_p of the vessel wall. Estimated values of L_p for both normal and tumour tissues vary widely. Direct measurements for individual tumour microvessels have not been reported, and estimates are based on indirect methods[59], However, evidence suggests that hydraulic conductivity is considerably higher in tumours than in normal tissues[59]. Representative values for normal and tumour tissues are 3.6 ×$10^{-8}$and 2.8 × 10^{-7} cms^{-1} $mmHg^{-1}$ respectively[13].

Transport through extravascular space.

As discussed above, transport of drugs through the extravascular space takes place by diffusion or convection, and penetration distance may be limited by rapid cellular uptake of the drug by tumour and normal cells that reside moderately close to microvessels. A number of structural and mechanical factors also limit drug penetration (FIG. 3). Many human tumours contain substantial amounts of ECM that surround nests (localized nodules of many tumour cells and associated normal cells). ECM is a transport barrier for several reasons: ECM can increase the diffusion distance for drug to reach target tumour cells; drugs can bind to ECM components, which reduces the amount of free drug available to reach tumour cells[60]; ECM can take up space[61,62] and present a steric barrier to diffusion of nanoparticles[62]; and ECM can be very dense, leading to collapse of tumour microvessels[63]. Stylianopoulos *et al.*[64] showed that stromal components (hyaluronic acid, collagen and fibroblasts) and tumour cells all contribute to compressive tissue stress in tumours. The uncontrolled proliferation of tumour cells may lead to regions of high cell density, reducing the width of the interstitial pathways for drug transport and increasing tortuosity of flow paths. Cell proliferation may also generate increased compressive tissue stresses, further contributing to collapse of tumour microvessels and preventing drug delivery[65].

As indicated in TABLE 1, several solute characteristics influence transport into tissue. Effects of solute diffusivity and uptake rate on tissue penetration have been discussed above. Another key parameter is the lipophilicity of the solute, often defined in terms of its octanol-to-water partition coefficient. Lipophilic solutes pass readily through cell membranes and can therefore take transcellular pathways through vessel walls and tissue. By contrast, hydrophilic solutes are restricted to aqueous paracellular pathways (between cells). In brain microvessels, the paracellular pathways are particularly restricted, and capillary permeability is closely correlated with the partition coefficient[66]. Experiments using a multicellular layer system have shown a positive dependence of the effective diffusion coefficient on the partition coefficient[67]. The partition coefficients of drugs used as payloads in nanotherapies vary widely, affecting both their binding to carriers and their free transport in tissue[68].

A major consequence of hyperpermeability of tumour microvessels and the relative lack of functional lymphatics is the accumulation of fluid and high interstitial fluid pressure (IFP). In normal tissues, the IFP is near zero or even slightly negative. In tumours, it can be in the range of 5–10 mmHg or higher[5], approaching intravascular pressure[37]. For macromolecules and nanoparticles, convection is normally the dominant transport mechanism in tissue (BOX 1). Elevated IFP can reduce the pressure gradient in interstitial space to near zero. The only transport process is then diffusion, which is very slow for macromolecules and nanoparticles[37].

Transport studies for drug design

Combining physical measurements of drug transport parameters with mathematical models can provide an improved basis for rational drug design. Examples of measurable parameters using intravital microscopy include vascular permeability[51,69] and the diffusion coefficient. Transport kinetics of free drug[54], macromolecules[70] and nanoparticles[52] have all been studied using intravital microscopy. Multicellular layer systems, combined with mathematical modelling of perfusion, diffusion and drug metabolic consumption rate, have proved valuable in the selection of small-molecule drugs with optimal transport properties[22,71]. Intravital microscopy studies in preclinical models that used nanoparticles of a range of sizes defined the importance of microvessel pore size in affecting nanoparticle drug delivery and showed that pore sizes varied depending on tumour type and location[52]. Nanoparticles are distinct from small molecules in that their size, shape, charge density and the extent of their water-soluble polymer coating (for example, polyethylene glycol) can affect circulation time and transport (TABLE 1). Consideration of these design features is important for rational nanoparticle drug design[72].

Methods to enhance drug delivery

In reviewing the extensive literature on methods to enhance drug delivery to tumours, we focus here on studies that have provided quantitative information on enhancement of drug concentrations and effectiveness in overcoming transport barriers. Also included are some studies addressing uniformity of drug delivery across a tumour and some human studies in which end points relevant to drug delivery were measured.

Inhibition of proangiogenic signalling.

The initial rationale for treatments based on inhibiting angiogenesis was that such treatments would inhibit tumour growth[73]. While this approach was not successful in human trials, antiangiogenic treatment by inhibition of VEGF signalling was found to be beneficial when given in combination with chemotherapy[74]. This seemingly paradoxical finding implied that inhibiting angiogenesis could lead to enhanced drug delivery. In response to this observation, Jain[37] proposed that inhibition of VEGF signalling can lead to 'normalization' of tumour vasculature and that this process can result in at least transient periods where perfusion and drug delivery are increased. The consequences of VEGF inhibition in tumours include reduction in the diameter of microvessels, pruning of the most immature vasculature, increased vascular maturity with increased pericyte coverage, reduced tortuosity[75] and reduction in IFP. However, it has not been definitively established that these changes are responsible for improved drug delivery. An alternative hypothesis[48] is that the inhibition of VEGF signalling leads to improved communication between endothelial cells via gap junctions, establishing upstream signalling by conducted responses and alleviating the problem of functional shunting (as described above). Vascular maturation is also driven by other cytokines and receptors, including platelet-derived growth factor B (PDGFB), PDGF receptor-β (PDGFRB)[76–78] and TIE2 (also known as TEK) (REFS 79,80), which may be suitable targets for improving vascular maturity and drug delivery in tumours[77,81].

In preclinical models and in patients with colorectal cancer, reductions in vascular density and/or increases in pericyte coverage have followed treatment with a range of strategies for VEGF inhibition[82–89]. More specifically, in preclinical models, changes in vascular density and maturity were correlated with a 1.25-fold to 3-fold increase in perfusion with the use of the VEGF antibody bevacizumab[87], endostatin and paclitaxel eluting nanoparticles[85,86], inhibitors of transforming growth factor-β (TGFβ) signalling[88] and metronomic dosing of 5-fluorouracil (5-FU)[90]; correlations between increased perfusion, drug delivery and improved response to chemotherapy were reported[85–88]. In a clinical study, improvements in perfusion were observed in 7/30 patients with recurrent glioblastoma treated with cediranib, a tyrosine kinase inhibitor of VEGF signalling[91]. Progression-free and overall survival were significantly improved in patients in whom tumour perfusion increased compared with those patients whose tumours exhibited no change or a reduction in perfusion. Similarly, improvement in K^{trans} was correlated with a histological response in patients with breast cancer who were treated preoperatively with a multi-receptor tyrosine kinase inhibitor (sunitinib) to normalize vasculature in combination with the chemotherapies doxorubicin and cyclophosphamide[84].

However, the use of VEGF inhibitors can also reduce perfusion and inhibit drug delivery, with potential for vascular rarefaction following long-term use[37]. A reduction in perfusion could lead to more hypoxia and reduced drug delivery[37,92]. Use of lower doses of these agents alleviates some of the deleterious effects of prolonged use of antiangiogenic agents[93].

Modification of IFP.

Reduction in vascular permeability lowers IFP, which can augment drug delivery, particularly for nanoparticles and drugs with M_r >1,000. Reductions in IFP have been

reported for a variety of angiogenesis inhibitors in preclinical models[82,83,94,95]. However, such treatment may also cause a reduction in microvascular pore sizes, reducing the transport of nanoparticles. Chauhan *et al.*[96] made a theroretical prediction that the reduction in pore sizes would be inhibitory for large nanoparticles but not for small ones near 10 nm in diameter. They demonstrated experimentally that uptake of protein-bound paclitaxel (l0 nm diameter) was augmented with VEGF inhibition, but uptake of liposomal doxorubicin (100 nm diameter) was not improved. Similarly, Tailor *et al.*[94] examined the transport of 100 nm liposomal doxorubicin in an A549 non-small-cell lung cancer (NSCLC) xenograft grown in nude mice following 7 days of treatment with the dual VEGF receptor 2 (VEGFR2) and PDGFRB antagonist pazopanib. In that study, treatment reduced vascular density and perivascular penetration of liposomes.

Arjaans *et al.*[89] examined tumour uptake of radio-labeled monoclonal antibodies by use of PET imaging at 24 hours and 144 hours after treatment of mice bearing SKOV-3 ovarian carcinoma xenografts or EO19 oesophageal carcinoma xenografts with bevacizumab. At both time points, uptake of antibodies was inhibited. Antibodies are similar in size to albumin (Stokes-Einstein radius 3.5–5 nm), and so these two types of protein have similar microvascular permeabilities and diffusivities[51]. In another independent mouse study, the VEGFR2 blocking antibody DC101 was shown to decrease vessel diameter, increase pericyte coverage and reduce IFP and vascular permeability to albumin twofold[83]. In spite of these effects, penetration distance from the microvasculature of fluorescently labelled albumin was nearly doubled because the increased pressure drop across the microvascular wall facilitated convective transport. The discrepancy between the results for antibodies and for albumin may result from the different binding characteristics of these proteins or from differences in experimental timing and end points.

Improvements in tumour perfusion by exercise.

Several preclinical reports indicate that sustained exercise can increase tumour perfusion[97–99] and vascular maturity[97]. These effects have been associated with improved drug delivery[100] and response to chemotherapy[97,100]. According to a recent report[100], the increase in vessel wall shear stress associated with increased blood flow rate during exercise activates calcineurin-nuclear factor of activated T cells, cytoplasmic 1 (NFATC1)-thrombospondin 1 (TSP1; also known as THBS1) signalling. TSP1 binds to VEGF to limit its bioavailability[101]. TSP1 also inhibits endothelial cell proliferation by binding to the CD36 receptor[102]. The reduction in VEGF activity combined with exercise-mediated chronic increase in shear stress results in more mature vasculature and higher overall perfusion[97–99]. An advantage of exercise is that its effects on perfusion are chronic, whereas the temporal window of effectiveness for antiangiogenic agents may be limited and difficult to determine. Jain and others[86,90,92] have recently emphasized that metronomic dosing of angiogenesis inhibitors may lead to prolonged normalization. In any case, strategies that can prolong the vascular normalization window for angiogenesis inhibitors need to be identified and rigorously tested. Furthermore, it would be of interest to determine whether the combination of exercise and angiogenesis inhibition yields a beneficial interaction.

Reduction of tissue stress by induction of tumour cell apoptosis.

In an approach termed ‘tumour priming’, tumour cell apoptosis is induced to enhance delivery of a second drug. Enhanced delivery occurs as a result of reduced tissue pressure, which opens collapsed vasculature and reduces IFP[64,103]. Drugs such as cyclophosphamide[104], paclitaxel[105,106] and taxanes[107] and those that target tumour necrosis factor (TNF)-related apoptosis-inducing ligand (TRAIL; also known as TNFSF10)[108] have successfully been used to prime tumours in mouse models. Induction of apoptosis decreased tumour cell density by 1.2-fold to 6-fold[104–108]. Nearly all studies reported an increase in the number of perfused microvessels (increased by 1.15-fold to 4-fold)[104–108], while IFP was also reported to be reduced[104,107,108]. Importantly, delivery of liposomal drugs was increased by 1.4-fold to 3-fold[104,108]; one report indicated a 1.5-fold increase in delivery of paclitaxel when a priming dose of the same drug was used 24 hours before a second dose[105]. In another report, priming by several apoptosis-inducing chemotherapies consistently improved monoclonal antibody uptake by 1.25-fold to 3-fold[107]. Moreover, tumour priming followed by a second chemotherapy was observed to prolong tumour regrowth time[104,106,108]. In the application of this approach, the relative timing of the treatments is likely to be an important issue as cell killing by apoptosis occurs over hours to days[109]. Imaging methods that are sensitive to changes in tumour cell density may prove useful in taking advantage of the priming effect[109,110].

Bypassing cellular drug resistance mechanisms.

Effective drug delivery to cancer cells can be impeded by ATP-binding cassette transporters that mediate drug efflux[111], which results in multidrug resistance. A doxorubicin-containing polymeric nanoparticle that contains a cleav-able hydrazine bond that releases the drug at a pH of 5.2 (equivalent to lysosomal pH) has been described[112,113]. This nanoparticle bypasses drug transporters because it is taken into cells by endocytosis. Drug release from this nanoparticle while inside the endosome minimizes direct interaction with drug pumps, such as p-glycoprotein. P-Glycoprotein is primarily located on the cell membrane[114], where it functions to pump drugs out of the cell[112]. Drug uptake in tumour cells was improved 4-fold to 5-fold compared with the same nanoparticle without the pH cleavable bond, and long-term control of tumour growth was observed in the syngeneic 4T1 mouse mammary tumour model and the MDA-MB-231 human breast tumour xenograft model[112]. Acid-cleavable bonds have also been used to release doxorubicin from elastin-like polypeptide drug carriers[115]. Here, longterm control of the CT26 mouse colon adenocarcinoma transplant model was observed.

Reducing ECM density to improve drug delivery.

Transport of macromolecules and nanoparticles through ECM depends on the fraction of space accessible to them[61], which is reduced by the presence of stromal fibres, such as collagen, and cells. The fraction of space is referred to as the extracellular volume fraction. In one study, in a rat MCA-R fibrosarcoma transplant model, the extracellular volume fraction averaged 20% for dextrans with an $M_r < 40{,}000$ but was well below 10% for larger dextrans[61]. By extrapolation, the extracellular volume fraction for nanoparticles would be even smaller as they are larger than dextrans. As a major component of ECM, hyaluronic

acid[116] is a glycosaminoglycan that can become crosslinked to various ECM components, contributing to the overall stiffness of the ECM layer. The enzyme hya-luronidase has been used to break down hyaluronic acid polymers in ECM, which lowers ECM stress, decompresses collapsed tumour microvessels[101,103] and lowers IFP[117]. These effects promote drug transport and motility of immune cells through tumour tissue[118]. A pegylated form of hyaluronidase improved delivery of gemcita-bine by 2-fold[116] and liposomal doxorubicin by 1.5-fold *in vivo* [117]. Specifically, enhancement of the antitumour effect with the enzyme compared with the drugs administered alone was reported in a transgenic mouse model that develops spontaneous pancreatic cancers (KPC, wherein endogenous mutant *Kras* and *Trp53* alleles are conditionally expressed in pancreatic cells) and two prostate tumour xenograft mouse models[116,117]. These effects occur most prominently in tumours with high hyaluronic acid content, such as pancreatic cancer[117,119]. In a recent report of a phase Ib trial, pegylated hyaluronidase increased K^{trans} in patients with metastatic pancreatic cancer[119]. In subset analysis, the longest surviving patients had the highest baseline content of hyaluronic acid in tumours.

Other promising approaches can also reduce tumour ECM. The pharmacological inhibition of Hedgehog signalling in a gemcitabine resistant, transgenic KPC pancreatic cancer model[120], was shown to double the fraction of perfused vessels and to double survival time compared with drug alone; specific pharmacological inhibition of PDGFRB signalling by use of STI-571 reduced IFP by 1.3-fold, in an anaplastic thyroid carcinoma xenograft model employing the human KAT-4 cell line. The reduction in IFP was associated with a 3-fold increase in accumulation of taxol and a significant delay in tumour growth[121]. The multi-tyrosine kinase inhibitor imatinib reduced IFP by 1.3-fold in a NSCLC xenograft model[122]. Target kinases whose inhibition may contribute to the effects of imatinib in promoting drug accumulation include PDGFR and the ABL kinase; the latter kinase influences TGFβ-mediated profibrotic pathways[123]. The local tumour control rate increased from 60% for docetaxel alone, to 100% with combined docetaxel and imatinib[95]. In line with its proangiogenic role[124], TGFβ inhibition in drug transport was evaluated with a function-blocking antibody in two different breast cancer mouse models and shown to lead to a reduction in overall microvascular density, which was accompanied by a slight increase in perfusion, a result that is consistent with vascular normalization[88]. Notably, penetration of doxorubicin-containing liposomes from the nearest blood vessel was increased by 2-fold[88]. A last example is the angiotensin II receptor antagonist losartan, which was demonstrated to reduce ECM component synthesis in several mouse tumour models (mammary, pancreatic fibrosarcoma and melanoma). The inhibition of ECM formation improved nanoparticle delivery by 1.5-fold to 4-fold, increasing antitumour effects by at least 2-fold compared with the administration of drug alone[125].

Use of normal cells to enhance drug delivery to tumours.

Although normal cell drug uptake is generally considered a barrier to drug transport efficiency, tumour-associated macrophages and stem cells have been harnessed for drug delivery[126,127]. For example, a systemically administered polymer-platinum prodrug nanoparticle was preferentially taken up by resident macrophages in an HT1080 fibrosarcoma xenograft in nude mice[127]. Slow drug release from these cells contributed to

the antitumour effect of this nanoparticle. At the experimental end point, tumours of animals treated with the nanoparticle were 2-fold smaller than control-treated tumours. Selective depletion of macrophages reduced drug uptake by 2-fold and abrogated the inhibition of tumour growth by the nanoparticle.

Effects of hyperthermia on nanoparticle drug transport.

Local or regional hyperthermia refers to a method for heating part of the body to temperatures between 40 °C and 45 °C[128]. Heating is typically achieved by use of radiofrequency, microwave or ultrasound applicators that deliver power into the target volume. Hyperthermia in the range of 41–43 °C increases microvascular permeability to albumin[129] and increases delivery of antibodies to D-54 glioma xenografts *in vivo* by 2-fold to 3-fold[130,131]. Hyperthermia also increases delivery of nanoparticles to tumours *in vivo*. The improvement in nanoparticle transport is related to increases in microvessel pore size[129], available extracellular volume fraction[132] and perfusion[133–137]. The average improvement in nanoparticle delivery with hyperthermia is in the range of 1.5-fold to 2-fold for a range of mouse tumour and xenograft models[138]. Heating to 42 °C increased doxorubicin uptake in subcutaneous FaDu squamous cell carcinoma xenografts in mice by 75% when sterically stabilized liposomal doxorubicin was used[139]. By comparison, hyperthermia did not improve free-drug delivery. The increase in endothelial gap size would not affect the transport of doxorubicin into the extravascular space because the transport of this small molecule is dominated by diffusion, not convection. The difference in drug delivery between free drug and liposomal drug with hyperthermia was 5-fold[138]. In another example, radiolabeled liposome uptake was increased 2-fold to 13-fold by hyperthermia in companion cats with vaccine-associated sarcomas[140]. Delivery of other nanoparticles can also be augmented by hyperthermia[141,142].

Mild ‘fever-range’ whole-body hyperthermia (39.5 °C for 4–6 hours) has been reported to decrease IFP[143], increase the fraction of perfused microvessels and increase liposomal doxorubicin uptake in tumours in a syngeneic CT26 mouse colorectal tumour model by nearly 3-fold, without any effect on drug uptake in the heart or kidney[144]. Moreover, an enhanced antitumour effect was observed with this combination of whole-body heating and with liposomal doxorubicin in the CT26 syngeneic mouse model as well as in two PDXs of colorectal origin[144].

Improvements in drug delivery are more pronounced when thermosensitive liposomes are used. Enhanced delivery occurs via intravascular drug release. The resultant high intravascular concentration drives drug into the tissue down its concentration gradient[54,145,146] (FIG. 4). A combined treatment regimen including hyperthermia at 42 °C and thermosensitive liposomes can increase drug delivery to tumours by 25-fold compared with administration of free drug, and by 5-fold over non-thermal-sensitive liposomes[139]. Hyperthermia-mediated increases in drug delivery yielded prolonged delays in tumour growth and achieved long-term local tumour control in several different mouse tumour and xenograft models[139,147–149]. The development of thermosensitive liposomes that exhibit rapid drug release in a modest hyperthermia temperature range (41–42°C)[150,151] has increased the feasibility for clinical application. One formulation has been tested in

humans[152,153] and is currently in phase I and phase III trials (NCT02112656 (REF. 154), NCT02181075 (REF. 155)).

Most of the studies discussed above used liposomal doxorubicin. A variety of other drugs have been encapsulated into thermosensitive liposomes, including cisplatin[156,157], methotrexate[158] andmelphalan[150]. An additional approach is to add an MR contrast agent or radionuclide to the liposomal formulation[160–162]. These dual formulations permit direct visualization of drug delivery. By use of MR-guided ultrasonography (to heat the tissue), drug delivery can be monitored in near real time[163–165].

Antibody-drug conjugates.

Antibody-drug conjugates (ADCs) are designed to achieve improved specificity for tumours by combining a potent cytotoxic drug (pay-load) with an antibody directed against an antigen that is preferentially expressed on tumour cells[166]. These two components are bridged by a linker that is typically stable in the circulation but cleaved when the drug is internalized by tumour cells. Owing to the complexity of such constructs, the chemical and biochemical aspects of their design have received much attention[167]; however, aspects related to the spatial distribution of the drug in tissues have received less emphasis. Given that ADCs have an M_r near 150,000, their penetration into tissue is limited[168]. Rapid binding of ADCs to antigen-positive cells near vessels can further limit their penetration distance into tissue. Their effectiveness therefore depends, to some extent, on the existence of the ‘bystander effect’ (REP. 169), according to which payload is released by antigen-positive cells exposed to the drug and can diffuse through the interstitial space to neighbouring antigennegative cells or to distant cells. Theoretical analyses can be used to study this effect[168,170] and may contribute to the development of successful ADCs. Numerous phase I and phase II clinical trials of ADCs are currently in progress[171]. It should be noted that the bystander effect may also contribute to the action of other categories of drugs discussed in this Review, including drug-loaded nanoparticles and prodrugs that are selectively activated, generating an active form of the drug that can diffuse to other regions of heterogeneous tumour tissues[22].

Conclusions

The identification of factors limiting drug delivery to cancer cells has stimulated a range of ingenious approaches to overcome these barriers and achieve enhanced drug delivery to solid tumours. Approaches based on angiogenesis inhibition, breakdown of ECM and tumour priming have yielded improvements in drug delivery in the range of 2-fold to 3-fold, which have correlated with improved antitumour effects. Physical methods to increase drug delivery, such as hyperthermia, have exhibited very large increases in drug delivery and consequent antitumour effects in animal models. Mild whole-body hyperthermia and partial-body hyperthermia have been reported to decrease IFP and increase drug delivery to mouse and human tumours, respectively[143,172]. Exercise has also proven to yield enhanced drug delivery and better antitumour effects.

The important question of whether the enhanced drug delivery to primary tumours achieved by these methods also extends to metastases remains somewhat unexplored at present. In

histological studies, vascular densities in human primary and metastatic renal cell carcinoma samples were found to be similar, suggesting that methods that increase drug delivery to a primary tumour also do so for metastases[173]. Strategies that enhance drug delivery in the primary tumour have been reported to reduce the incidence of metastases, but these effects may be the result of reduced tumour cell shedding from the primary tumour, whose growth was inhibited[174,175]. The effects of hyperthermia are largely restricted to the heated tumour, and it is unclear how such treatment could affect metastases. However, local heating has been reported to increase antibody[131] and liposomal drug delivery to distant, unheated sites, where they can inhibit tumour growth[176].

The delivery of adequate concentrations of anticancer agents to all cancer cells in solid tumours is strongly dependent on the structure and function of the vasculature and on drug transport properties in tissue. Until now, relatively few investigators (notably Jain and colleagues) have focused attention on these aspects of cancer treatment. Over the past several decades, the basic principles governing solute transport to tumours have been established, and a number of methods have been developed to overcome barriers to drug delivery. At the same time, the challenges involved in delivering drugs effectively throughout tumours have become increasingly evident. The intertumoural and intratumoural heterogeneities in tumour properties lead to highly variable efficiency in drug delivery. The large number of interacting physical, chemical and biological factors that determine drug distribution complicate efforts to design effective strategies. Future progress in this field is likely to depend increasingly on the combination of spatially resolved experimental observations of transport parameters and theoretical models for transport processes and cellular responses. For example, transport-related parameters derived from dynamic contrast-enhanced MRI (DCE-MRI) and contrast imaging parameters from computed tomography (CT), such as texture analysis[177] using principal component analysis, change in T1 relaxivity[160], blood volume fraction[178] and area under the curve[179], have been correlated with drug uptake and/or treatment response in both murine and human tumours. Increased understanding of drug transport processes and consideration of these processes in the design and usage of drugs has the potential to result in improved treatment methods for solid tumours.

Acknowledgements

This work was supported by National Institutes of Health (NIH) grants CA040355 and HL034555.

References

1. Bast RC et al. Holland-Frei Cancer Medicine 9th *edn* Wiley-Blackwell, 2017).
2. Swabb EA, Wei J & Gullino PM Diffusion and convection in normal and neoplastic tissues. Cancer Res 34, 2814–2822 (1974). [PubMed: 4369924] In this early account of how tissue glycosaminoglycan content can affect solute transport by convection compared with by diffusion in tumours, the authors suggest that degradation of glycosaminoglycan with hyaluronidase could improve solute transport in tumours.
3. Jain RK Transport of molecules across tumor vasculature. Cancer Metastasis Rev 6, 559–593 (1987). [PubMed: 3327633] This comprehensive review discusses the transport properties of microvessel walls with respect to their importance for drugs of various sizes.

4. Jain RK Transport of molecules in the tumor interstitium: a review. Cancer Res 47, 3039–3051 (1987). [PubMed: 3555767] This review focuses on factors that impede solute transport in the interstitium of tumours and shows how high IFP and lack of functioning lymphatics contribute to reduced transport.
5. Jain RK The Eugene M. Landis Award Lecture 1996. Delivery of molecular and cellular medicine to solid tumors. Microcirculation 4, 1–23 (1997). [PubMed: 9110280]
6. Chauhan VP, Stylianopoulos T, Boucher Y & Jain RK Delivery of molecular and nanoscale medicine to tumors: transport barriers and strategies. Annu. Rev. Chem. Biomol. Eng 2, 281–298 (2011). [PubMed: 22432620]
7. Chauhan VP & Jain RK Strategies for advancing cancer nanomedicine. Nat. Mater 12, 958–962 (2013). [PubMed: 24150413]
8. El-Kareh AW & Secomb TW Theoretical models for drug delivery to solid tumors. Crit. Rev. Biomed. Eng 25,503–571 (1997). [PubMed: 9719859]
9. Ribatti D, Nico B, Crivellato E & Vacca A The structure of the vascular network of tumors. Cancer Lett 248, 18–23 (2007). [PubMed: 16879908]
10. Maeda H, Wu J, Sawa T, Matsumura Y & Hori K Tumor vascular permeability and the EPR effect in macromolecular therapeutics: a review. J. Control. Release 65, 271–284 (2000). [PubMed: 10699287] This review discusses the features that enhance large drug and nanoparticle transport to tumours (the EPR effect) and the roles of VEGF, nitric oxide and other vasoactive and pro-angiogenic factors in these processes.
11. Minchinton AI & Tannock IF Drug penetration in solid tumours. Nat. Rev. Cancer 6, 583–592 (2006). [PubMed: 16862189] This Review examines the features of the tumour microenvironment that inhibit small molecule transport and illustrates that the barriers are substantial, even for small drugs.
12. Chary SR & Jain RK Direct measurement of interstitial convection and diffusion of albumin in normal and neoplastic tissues by fluorescence photobleaching. Proc. Natl Acad. Sci. USA 86, 5385–5389 (1989). [PubMed: 2748592]
13. Baxter LT & Jain RK Transport of fluid and macromolecules in tumors. I. Role of interstitial pressure and convection. Microvasc. Res 37, 77–104 (1989). [PubMed: 2646512]
14. Levick JR An Introduction to Cardiovascular Physiology 4th edn (Hodder Arnold, 2003).
15. Pardridge WM The blood-brain barrier: bottleneck in brain drug development. NeuroRx 2, 3–14 (2005). [PubMed: 15717053]
16. Primeau AJ, Rendon A, Hedley D, Lilge L & Tannock IF The distribution of the anticancer drug doxorubicin in relation to blood vessels in solid tumors. Clin. Cancer Res 11,8782–8788 (2005). [PubMed: 16361566]
17. Dewhirst MW, Cao Y & Moeller B Cycling hypoxia and free radicals regulate angiogenesis and radiotherapy response. Nat. Rev. Cancer 8, 425–437 (2008). [PubMed: 18500244]
18. Wilson WR & Hay MP Targeting hypoxia in cancer therapy. Nat. Rev. Cancer 11,393–410 (2011). [PubMed: 21606941]
19. Thomlinson RH & Gray LH The histological structure of some human lung cancers and the possible implications for radiotherapy. Br. J. Cancer 9, 539–549 (1955). [PubMed: 13304213]
20. Vaupel P & Mayer A Hypoxia in cancer: significance and impact on clinical outcome. Cancer Metastasis Rev 26, 225–239 (2007). [PubMed: 17440684]
21. Brown JM & Giaccia AJ Tumour hypoxia: the picture has changed in the 1990s. Int. J. Radiat. Biol 65,95–102 (1994). [PubMed: 7905916]
22. Hicks KO et al. Use of three-dimensional tissue cultures to model extravascular transport and predict *in vivo* activity of hypoxia-targeted anticancer drugs. J. Natl Cancer Inst 98, 1118–1128 (2006). [PubMed: 16912264]
23. Baish JW et al. Scaling rules for diffusive drug delivery in tumor and normal tissues. Proc. Natl Acad. Sci. USA 108, 1799–1803 (2011). [PubMed: 21224417]
24. El-Kareh AW & Secomb TW A theoretical model for intraperitoneal delivery of cisplatin and the effect of hyperthermia on drug penetration distance. Neoplasia 6, 117–127 (2004). [PubMed: 15140400]

25. Senger DR et al. Tumor-cells secrete a vascular-permeability factor that promotes accumulation of ascites-fluid. Science 219, 983–985 (1983). [PubMed: 6823562]
26. Dewhirst MW & Ashcraft KA Implications of increase in vascular permeability in tumors by VEGF: a commentary on the pioneering work of Harold Dvorak. Cancer Res 76,3118–3121 (2016). [PubMed: 27251086]
27. Sevick EM & Jain RK Geometric resistance to blood flow in solid tumors perfused *ex vivo* — effects of tumor size and perfusion pressure. Cancer Res 49, 3506–3512 (1989). [PubMed: 2731172]
28. Sevick EM & Jain RK Viscous resistance to blood flow in solid tumors — effect of hematocrit on intratumor blood viscosity. Cancer Res 49, 3513–3519 (1989). [PubMed: 2731173]
29. Dewhirst MW et al. Effects of the calcium-channel blocker flunarizine on the hemodynamics and oxygenation of tumor microvasculature. Radiat. Res 132, 61–68 (1992). [PubMed: 1410275]
30. Kavanagh BD, Coffey BE, Needham D, Hochmuth RM & Dewhirst MW The effect of flunarizine on erythrocyte suspension viscosity under conditions of extreme hypoxia, low pH, and lactate treatment. Br.J. Cancer 67, 734–741 (1993). [PubMed: 8471430]
31. Falk P Patterns of vasculature in 2 pairs of related fibrosarcomas in rat and their relation to tumor responses to single large doses of radiation. Eur. J. Cancer 14, 237–250 (1978). [PubMed: 631174]
32. Dewhirst MW et al. Quantification of longitudinal tissue po_2 gradients in window chamber tumours: impact on tumour hypoxia. Br J. Cancer 79, 1717–1722 (1999). [PubMed: 10206282]
33. Less JR, Skalak TC, Sevick EM & Jain RK Microvascular architecture in a mammary-carcinoma — branching patterns and vessel dimensions. Cancer Res 51,265–273 (1991). [PubMed: 1988088]
34. Mayrovitz HN & Roy J Microvascular blood flow: evidence indicating a cubic dependence on arteriolar diameter. Am. J. Physiol 245, H1031–H1038 (1983). [PubMed: 6660303]
35. Dewhirst MW et al. Morphologic and hemodynamic comparison of tumor and healing normal tissue microvasculature. Int. J. Radiat. Oncol. Biol. Phys 17, 91–99 (1989). [PubMed: 2745213]
36. Secomb TW, Hsu R, Dewhirst MW, Klitzman B & Gross JF Analysis of oxygen transport to tumor tissue by microvascular networks. Int. J. Radiat. Oncol. Biol. Phys 25, 481–489 (1993). [PubMed: 8436527] This study uses a mathematical model to show that the irregular structure of tumour microcirculation leads to a wide distribution of tissue oxygen levels, implying that heterogeneous responses to radiation and some types of chemotherapy can be dependent on hypoxia.
37. Jain RK Normalization of tumor vasculature: an emerging concept in antiangiogenic therapy. Science 307, 58–62 (2005). [PubMed: 15637262] This commentary proposes a novel rationale for the use of antiangiogenic drugs; namely, that enhanced drug delivery could occur because of pruning of nonfunctional microvasculature coupled with a reduction in the diameter of remaining vasculature.
38. Winkler F et al. Kinetics of vascular normalization by VEGFR2 blockade governs brain tumor response to radiation: role of oxygenation, angiopoietin-1, and matrix metalloproteinases. Cancer Cell 6, 553–563 (2004). [PubMed: 15607960]
39. Dewhirst MW et al. Perivascular oxygen tensions in a transplantable mammary tumor growing in a dorsal flap window chamber. Radiat. Res 130, 171–182 (1992). [PubMed: 1574573]
40. Helmlingei G, Yuan F, Dellian M & Jain RK Interstitial pH and po2 gradients in solid tumors *in vivo:* high-resolution measurements reveal a lack of correlation. Nat. Med 3, 177–182 (1997). [PubMed: 9018236]
41. Kimura H et al. Fluctuations in red cell flux in tumor microvessels can lead to transient hypoxia and reoxygenation in tumor parenchyma. Cancer Res 56, 5522–5528(1996). [PubMed: 8968110]
42. Dewhirst MW Relationships between cycling hypoxia, HIF-1, angiogenesis and oxidative stress. Radiat. Res 172, 653–665 (2009). [PubMed: 19929412]
43. Sorg BS, Hardee ME, Agarwal N, Moeller BJ & Dewhirst MW Spectral imaging facilitates visualization and measurements of unstable and abnormal microvascular oxygen transport in tumors. J. Biomed. Opt 13,014026(2008). [PubMed: 18315384]
44. Yeh CH et al. Optical-resolution photoacoustic microscopy of the metabolic rate of oxygen in a mouse renal tumor model. Proc. SPIE 9323, 93233H (2015).
45. Feindel W & Perot P Red cerebral veins — a report on arteriovenous shunts in tumors and cerebral scars. J. Neurosurg 22, 315–325 (1965). [PubMed: 14318107]

46. Forman WH, Green JD & Oberheu V Arteriovenous shunting in renal pelvic tumors. South. Med. J 68, 992–993 (1975). [PubMed: 1162415]
47. Numata K et al. Flow characteristics of hepatic-tumors at color Doppler sonography — correlation with arteriographic findings. Am. J. Roentgenol 160, 515–521 (1993). [PubMed: 8381573]
48. Pries AR, Hopfner M, le Noble F, Dewhirst MW & Secomb TW The shunt problem: control of functional shunting in normal and tumour vasculature. Nat. Rev. Cancer 10, 587–593 (2010). [PubMed: 20631803] This Opinion article proposes that signal propagation along walls of blood vessels is impaired in tumours, resulting in dysfunctional microcirculation, and that antiangiogenic treatment may restore vascular communication and thereby normalize vascular function.
49. Pries AR, Secomb TW & Gaehtgens P Structural adaptation and stability of microvascular networks: theory and simulations. Am. J. Physiol 275, H349–H360 (1998). [PubMed: 9683420]
50. Figueroa XF & Duling BR Gap junctions in the control of vascular function. Antioxid. Redox Signal 11,251–266 (2009). [PubMed: 18831678]
51. Yuan F et al. Vascular-permeability in a human tumor xenograft - molecular-size dependence and cutoff size. Cancer Res 55, 3752–3756 (1995). [PubMed: 7641188]
52. Yuan F et al. Microvascular permeability and interstitial penetration of sterically stabilized (stealth) liposomes in a human tumor xenograft. Cancer Res 54,3352–3356 (1994). [PubMed: 8012948] This first report of permeability coefficient measurements for nanoparticles (sterically stabilized liposomes) in tumour tissue compared with normal tissue shows that extravasated liposomes remain in the perivascular space for many days.
53. Yokoi K et al. Capillary-wall collagen as a biophysical marker of nanotherapeutic permeability into the tumor microenvironment. Cancer Res 74, 4239–4246 (2014). [PubMed: 24853545]
54. Manzoor AA et al. Overcoming limitations in nanoparticle drug delivery: triggered, intravascular release to improve drug penetration into tumors. Cancer Res 72, 5566–5575 (2012). [PubMed: 22952218] This report outlines a strategy to increase drug transport to tumours more efficiently than through the EPR effect by use of hyperthermia to achieve thermosensitive liposomal drug release within the tumour vasculature.
55. Miller MA et al. Predicting therapeutic nanomedicine efficacy using a companion magnetic resonance imaging nanoparticle. Sci. Transl Med 7, 314ra 183 (2015).
56. Bertrand N, Wu J, Xu X, Kamaly N & Farokhzad OC Cancer nanotechnology: the impact of passive and active targeting in the era of modern cancer biology. Adv. DrugDeliv. Rev 66, 2–25 (2014).
57. Lee H et al. ^{64}Cu-MM-302 positron emission tomography quantifies variability of enhanced permeability and retention of nanoparticles in relation to treatment response in patients with metastatic breast cancer. Clin. Cancer Res 23, 4190–4202 (2017). [PubMed: 28298546]
58. Prabhakar U et al. Challenges and key considerations of the enhanced permeability and retention effect for nanomedicine drug delivery in oncology. Cancer Res 73,2412–2417 (2013). [PubMed: 23423979]
59. Sevick EM & Jain RK Measurement of capillary filtration coefficient in a solid tumor. Cancer Res 51, 1352–1355 (1991). [PubMed: 1997172]
60. Chang Q et al. Biodistribution of cisplatin revealed by imaging mass cytometry identifies extensive collagen binding in tumor and normal tissues. Sci. Rep 6, 36641 (2016). [PubMed: 27812005]
61. Krol A, Maresca J, Dewhirst MW & Yuan F Available volume fraction of macromolecules in the extravascular space of a fibrosarcoma: implications for drug delivery. Cancer Res 59, 4136–4141 (1999). [PubMed: 10463619]
62. Yuan F, Krol A & Tong S Available space and extracellular transport of macromolecules: effects of pore size and connectedness. Ann. Biomed. Engineer 29, 1150–1158 (2001).This study shows that collapse of tumour microvessels is not the result of high IFP, but that the hyaluronic acid component of tumour ECM plays a role in compressing microvessels.
63. Provenzano PP et al. Enzymatic targeting of the stroma ablates physical barriers to treatment of pancreatic ductal adenocarcinoma. Cancer Cell 21, 418–429 (2012). [PubMed: 22439937]
64. Stylianopoulos T et al. Causes, consequences, and remedies for growth-induced solid stress in murine and human tumors. Proc. Natl Acad. Sci. USA 109, 15101–15108 (2012). [PubMed: 22932871]

65. Chauhan VP et al. Compression of pancreatic tumor blood vessels by hyaluronan is caused by solid stress and not interstitial fluid pressure. Cancer Cell 26, 14–15 (2014). [PubMed: 25026209]
66. Levin VA Relationship of octanol/water partition coefficient and molecular weight to rat brain capillary permeability. J. Med. Chem 23, 682–684 (1980). [PubMed: 7392035]
67. Pruijn FB, Patel K Hay MP, Wilson WR & Hicks KO Prediction of tumour tissue diffusion coefficients of hypoxia-activated prodrugs from physicochemical parameters. Aust. J. Chem 61, 687–693 (2008).
68. Norvaisas P & Ziemys A The role of payload hydrophobicity in nanotherapeutic pharmacokinetics. J. Pharrn. Sci 103,2147–2156 (2014).
69. Wu NZ et al. Increased microvascular permeability contributes to preferential accumulation of Stealth liposomes in tumor tissue. Cancer Res 53, 3765–3770 (1993). [PubMed: 8339289]
70. Dreher MR et al. Tumor vascular permeability, accumulation, and penetration of macromolecular drug carriers. J. Natl Cancer Inst 98, 335–344 (2006). [PubMed: 16507830] This is the first paper to systematically evaluate the size dependence of macromolecular transport across tumour microvasculature and into the interstitial space.
71. Kyle AH, Huxham LA, Chiam AS, Sim DH & Minchinton AI Direct assessment of drug penetration into tissue using a novel application of three-dimensional cell culture. Cancer Res 64, 6304–6309 (2004). [PubMed: 15342419]
72. Stylianopoulos T & Jain RK Design considerations for nanotherapeutics in oncology. Nanomedicine 11, 1893–1907 (2015). [PubMed: 26282377]
73. Folkman J Tumor angiogenesis: therapeutic implications. N. Engl. J. Med 285, 1182–1186 (1971). [PubMed: 4938153]
74. Hurwitz H et al. Bevacizumab plus irinotecan, fluorouracil, and leucovorin for metastatic colorectal cancer. N. Engl.J. Med 350, 2335–2342 (2004). [PubMed: 15175435]
75. Yuan F et al. Time-dependent vascular regression and permeability changes in established human tumor xenografts induced by an anti-vascular endothelial growth factor vascular permeability factor antibody. Proc. Natl Acad. Sci. USA 93, 14765–14770 (1996). [PubMed: 8962129]
76. Jain RK & Booth MF What brings pericytes to tumor vessels? J. Clin. Invest 112, 1134–1136 (2003). [PubMed: 14561696]
77. Abramsson A, Lindblom P & Betsholtz C Endothelial and nonendothelial sources of PDGF-B regulate pericyte recruitment and influence vascular pattern formation in tumors. J. Clin. Invest 112, 1142–1151 (2003). [PubMed: 14561699]
78. Hellstrom M, Kalen M, Lindahl P, Abramsson A & Betsholtz C Role of PDGF-B and PDGFR-beta in recruitment of vascular smooth muscle cells and pericytes during embryonic blood vessel formation in the mouse. Development 126, 3047–3055 (1999). [PubMed: 10375497]
79. Lin PN et al. Inhibition of tumor angiogenesis using a soluble receptor establishes a role for Tie2 in pathologic vascular growth. J. Clin. Invest 100, 2072–2078 (1997). [PubMed: 9329972]
80. Wong AL et al. Tie2 expression and phosphorylation in angiogenic and quiescent adult tissues. Circul. Res 81,567–574 (1997).
81. Goel S et al. Effects of vascular-endothelial protein tyrosine phosphatase inhibition on breast cancer vasculature and metastatic progression. J.Natl Cancer Inst 105, 1188–1201 (2013). [PubMed: 23899555]
82. Willett CG et al. Direct evidence that the VEGF-specific antibody bevacizumab has antivascular effects in human rectal cancer. Nat. Med 10, 145–147 (2004). [PubMed: 14745444] This study demonstrates potent antiangiogenic effects of bevacizumab in human patients with rectal cancer and suggests that the tumour vasculature became more efficient after treatment.
83. Tong RT et al. Vascular normalization by vascular endothelial growth factor receptor 2 blockade induces a pressure gradient across the vasculature and improves drug penetration in tumors. Cancer Res 64, 3731–3736(2004). [PubMed: 15172975]
84. Wong ALA et al. Phase Ib/II randomized, open-label study of doxorubicin and cyclophosphamide with or without low-dose, short-course sunitinib in the pre-operative treatment of breast cancer. Oncotarget 7, 64089–64099 (2016). [PubMed: 27577069]

85. Li W et al. Gold nanoparticle-mediated targeted delivery of recombinant human endostatin normalizes tumour vasculature and improves cancer therapy. Sci. Rep 6, 11 (2016). [PubMed: 28442704]
86. Luan X et al. Tumor priming using metronomic chemotherapy with neovasculature-targeted, nanoparticulate paclitaxel. Biomaterials 95, 60–73 (2016). [PubMed: 27130953]
87. Dickson PV et al. Revacizumab-induced transient remodeling of the vasculature in neuroblastoma xenografts results in improved delivery and efficacy of systemically administered chemotherapy. Clin. Cancer Res 13, 3942–3950 (2007). [PubMed: 17606728]
88. Liu JQ et al. TGF-β blockade improves the distribution and efficacy of therapeutics in breast carcinoma by normalizing the tumor stroma. Proc. Natl Acad. Sci. USA 109, 16618–16623 (2012). [PubMed: 22996328]
89. Arjaans M et al. Bevacizumab-induced normalization of blood vessels in tumors hampers antibody uptake. Cancer Res 73, 3347–3355 (2 013). [PubMed: 23580572]
90. Doi Y et al. Improvement of intratumor microdistribution of PEGylated liposome via tumor priming by metronomic S-l dosing. Int. J. Nanomed 11,5573–5582 (2016).
91. Sorensen AG et al. Increased survival of glioblastoma patients who respond to antiangiogenic therapy with elevated blood perfusion. Cancer Res 72 402–407 (2012). [PubMed: 22127927]
92. Jain RK Normalizing tumor microenvironment to treat cancer: bench to bedside to biomarkers. J. Clin. Oncol 31,2205–2218 (2013). [PubMed: 23669226]
93. Jain RK Antiangiogenesis strategies revisited: from starving tumors to alleviating hypoxia. Cancer Cell 26, 605–622 (2014). [PubMed: 25517747]
94. Tailor TD et al. Effect of pazopanib on tumor microenvironment and liposome delivery. Mol. Cancer Ther 9, 1798–1808 (2010). [PubMed: 20515941]
95. Vlahovic G, Rabbani ZN, Herndon JE, Dewhirst MW & Vujaskovic Z Treatment with Imatinib in NSCLC is associated with decrease of phosphorylated PDGFR-β and VEGF expression, decrease in interstitial fluid pressure and improvement of oxygenation. Br. J. Cancer 95, 1013–1019 (2006). [PubMed: 17003785]
96. Chauhan VP et al. Normalization of tumour blood vessels improves the delivery of nanomedicines in a size-dependent manner. Nat. Nanotechnol 7, 383–388 (2012). [PubMed: 22484912]
97. Betof AS et al. Modulation of murine breast tumor vascularity, hypoxia, and chemotherapeutic response by exercise. J. Natl Cancer Inst 107, djv040 (2 015). [PubMed: 25780062]
98. Jones LW et al. Exercise modulation of the host-tumor interaction in an orthotopic model of murine prostate cancer. J. Appl. Physiol 113, 263–272 (2012). [PubMed: 22604887]
99. Jones LW et al. Effect of aerobic exercise on tumor physiology in an animal model of human breast cancer. J. Appl. Physiol 108, 343–348 (2010). [PubMed: 19959769]
100. Schadler KL et al. Tumor vessel normalization after aerobic exercise enhances chemotherapeutic efficacy. Oncotarget 7, 65429–65440 (2016). [PubMed: 27589843]
101. Greenaway J et al. Thrombospondin-1 inhibits VEGF levels in the ovary directly by binding and internalization via the low density lipoprotein receptor-related protein-1 (LRP-1). J. Cell. Physiol 210, 807–818(2007). [PubMed: 17154366]
102. Edwards AK, Olariu I, Nakamura DS, Ahn SH & Tayade C Chronic effects of an anti-angiogenic thrombospondin-1 mimetic peptide, ABT-898, on female mouse reproductive outcomes. Reprod. Biol. Endocrinol 14, 10 (2016). [PubMed: 26936606]
103. Griffon-Etienne G, Boucher Y, Brekken C, Suit HD & Jain RK Taxane-induced apoptosis decompresses blood vessels and lowers interstitial fluid pressure in solid tumors: clinical implications. Cancer Res 59, 3776–3782 (1999). [PubMed: 10446995]
104. Geretti E et al. Cyclophosphamide-mediated tumor priming for enhanced delivery and antitumor activity of HER2-targeted liposomal doxorubicin (MM-302). Mol. Cancer Ther 14,2060–2071 (2015). [PubMed: 26162690]
105. Jang SH, Wientjes MG & Au JLS Enhancement of paclitaxel delivery to solid tumors by apoptosis-inducing pretreatment: effect of treatment schedule. J. Pharmacol. Exp. Ther 296, 1035–1042 (2001). [PubMed: 11181938]
106. Lu D, Wientjes MG Lu Z & Au JLS Tumor priming enhances delivery and efficacy of nanomedicines. J. Pharmacol. Exp. Ther 322, 80–88 (2007). [PubMed: 17420296]

107. Jang JK et al. Cytoreductive chemotherapy improves the biodistribution of antibodies directed against tumor necrosis in murine solid tumor models. Mol. Cancer Ther 12, 2827–2836 (2013). [PubMed: 24130055]
108. Hylander BL et al. Tumor priming by Apo2L/TRAIL reduces interstitial fluid pressure and enhances efficacy of liposomal gemcitabine in a patient derived xenograft tumor model. J. Control. Release 217, 160–169 (2015). [PubMed: 26342663]
109. Edgington LE et al. Noninvasive optical imaging of apoptosis by caspase-targeted activity-based probes. Nat. Med 15, 967–973 (2009). [PubMed: 19597506]
110. Lee KC et al. Prospective early response imaging biomarker for neoadjuvant breast cancer chemotherapy. Clin. Cancer Res 13, 443–450 (2007). [PubMed: 17255264]
111. Szakacs G, Paterson JK, Ludwig JA, Booth-Genthe C & Gottesman MM Targeting multidrug resistance in cancer. Nat. Rev. Drug Discov 5,219–234 (2006). [PubMed: 16518375]
112. Xu R et al. An injectable nanoparticle generator enhances delivery of cancer therapeutics. Nat. Biotechnol 34, 414–418 (2016). [PubMed: 26974511]
113. Geisow MJ, D'Arcy Hart P & Young MR Temporal changes of lysosome and phagosome pH during phagolysosome formation in macrophages: studies by fluorescence spectroscopy. J. Cell Biol 89, 645–652 (1981). [PubMed: 6166620]
114. Thiebaut F et al. Cellular localization of the multidrug-resistance gene product P-glycoprotein in normal human tissues. Proc. Natl Acad. Sci. USA 84, 7735–7738 (1987). [PubMed: 2444983]
115. MacKay JA et al. Self-assembling chimeric polypeptide-doxorubicin conjugate nanoparticles that abolish tumours after a single injection. Nat. Mater 8, 993–999 (2009). [PubMed: 19898461]
116. Jacobetz MA et al. Hyaluronan impairs vascular function and drug delivery in a mouse model of pancreatic cancer. Gut 62, 112–120 (2013). [PubMed: 22466618]
117. Thompson CB et al. Enzymatic depletion of tumor hyaluronan induces antitumor responses in preclinical animal models. Mol. Cancer Ther 9, 3052–3064 (2010). [PubMed: 20978165]
118. Singha NC et al. Tumor-associated hyaluronan limits efficacy of monoclonal antibody therapy. Mol. Cancer Ther 14, 523–532 (2015). [PubMed: 25512619]
119. Hingorani SR et al. Phase Ib study of PEGylated recombinant human hyaluronidase and gemcitabine in patients with advanced pancreatic cancer. Clin. Cancer Res 22, 2848–2854 (2016). [PubMed: 26813359] This is the first clinical evaluation of the use of hyaluronidase to enhance drug delivery to pancreatic cancer.
120. Olive KP et al. Inhibition of Hedgehog signaling enhances delivery of chemotherapy in a mouse model of pancreatic cancer. Science 324, 1457–1461 (2009). [PubMed: 19460966]
121. Pietras K et al. Inhibition of platelet-derived growth factor receptors reduces interstitial hypertension and increases transcapillary transport in tumors. Cancer Res 61,2929–2934 (2001). [PubMed: 11306470]
122. Vlahovic G et al. Treatment with imatinib improves drug delivery and efficacy in NSCLC xenografts. Br.J. Cancer 97, 735–740 (2007). [PubMed: 17712313]
123. Lee SJ & Wang JYJ Exploiting the promiscuity of imatinib BMC Biol 8, 30 (2010). [PubMed: 20370908]
124. Pardali E & ten Dijke P Transforming growth factor-β signaling and tumor angiogenesis. Front. Biosci 14, 4848–4861 (2009).
125. Diop-Frimpong B, Chauhan VP, Krane S, Boucher Y & Jain RK Losartan inhibits collagen I synthesis and improves the distribution and efficacy of nanotherapeutics in tumors. Proc. Natl Acad. Sci. USA 108,2909–2914 (2011). [PubMed: 21282607]
126. Bago JR et al. Therapeutically engineered induced neural stem cells are tumour-homing and inhibit progression of glioblastoma. Nat. Commun 7, 10593 (2016). [PubMed: 26830441]
127. Miller MA et al. Tumour-associated macrophages act as a slow-release reservoir of nano-therapeutic Pt(IV) pro-drug. Nat. Commun 6, 8692 (2015). [PubMed: 26503691]
128. Dewhirst M, Stauffer P, Das S, Craciunescu O & Vujaskovic Z in Clinical Radiation Oncology (eds Gunderson L & Tepper J) 381–398 (Elsevier, 2016).
129. Kong G, Braun RD & Dewhirst MW Hyperthermia enables tumor-specific nanoparticle delivery: effect of particle size. Cancer Res 60, 4440–4445 (2000). [PubMed: 10969790] This study

demonstrates that hyperthermia increases pore sizes in tumour microvessels, which yields enhanced nanoparticle delivery.

130. Cope DA, Dewhirst MW, Friedman HS, Bigner DD & Zalutsky MR Enhanced delivery of a monoclonal-antibody F(ab')$_2$ fragment to subcutaneous human glioma xenografts using local hyperthermia. Cancer Res 50, 1803–1809 (1990). [PubMed: 2407344]
131. Schuster JM et al. Hyperthermic modulation of radiolabeled antibody uptake in a human glioma xenograft and normal tissues. Int. J. Hyperthermia 11, 59–72 (1995). [PubMed: 7714371]
132. Krol A, Dewhirst MW & Yuan F Effects of cell damage and glycosaminoglycan degradation on available extravascular space of different dextrans in a rat fibrosarcoma. Int. J. Hyperthermia 19, 154–164 (2003). [PubMed: 12623638]
133. Dudar TE & Jain RK Differential response of normal and tumor microcirculation to hyperthermia. Cancer Res 44, 605–612 (1984). [PubMed: 6692365]
134. Song CW Effect of local hyperthermia on blood flow and microenvironment — a review Cancer Res 44, 4721–4730 (1984).
135. Song CW, Rhee JG & Levitt SH Blood flow in normal tissues and tumors during hyperthermia. J. Natl Cancer Inst 64, 119–124 (1980). [PubMed: 6928036]
136. Meyer RE, Braun RD, Rosner GL & Dewhirst MW Local 42 degrees C hyperthermia improves vascular conductance of the R3230Ac rat mammary adenocarcinoma during sodium nitroprusside infusion. Radiat. Res 154, 196–201 (2000). [PubMed: 10931692]
137. Vujaskovic Z et al. Temperature-dependent changes in physiologic parameters of spontaneous canine soft tissue sarcomas after combined radiotherapy and hyperthermia treatment. Int J. Radiat. Oncol. Biol. Phys 46, 179–185 (2000). [PubMed: 10656391]
138. Kong G & Dewhirst MW Hyperthermia and liposomes. Int. J. Hyperthermia 15, 345–370 (1999). [PubMed: 10519688]
139. Kong G et al. Efficacy of liposomes and hyperthermia in a human tumor xenograft model: Importance of triggered drug release. Cancer Res 60, 6950–6957 (2000). [PubMed: 11156395]
140. Matteucci ML et al. Hyperthermia increases accumulation of technetium-99m-labeled liposomes in feline sarcomas. Clin. Cancer Res 6, 3748–3755 (2000). [PubMed: 10999769]
141. McDaniel JR, Dewhirst MW & Chilkoti A Actively targeting solid tumours with thermoresponsive drug delivery systems that respond to mild hyperthermia. Int. J. Hyperthermia 29, 501–510 (2013). [PubMed: 23924317]
142. McDaniel JR et al. Rational design of "heat seeking" drug loaded polypeptide nanoparticles that thermally target solid tumors. Nano Lett 14, 2890–2895 (2014). [PubMed: 24738626]
143. Winslow TB et al. A pilot study of the effects of mild systemic heating on human head and neck tumour xenografts: analysis of tumour perfusion, interstitial fluid pressure, hypoxia and efficacy of radiation therapy. Int. J. Hyperthermia 31,693–701 (2015). [PubMed: 25986432]
144. Xu Y et al. Fever-range whole body hyperthermia increases the number of perfused tumor blood vessels and therapeutic efficacy of liposomally encapsulated doxorubicin. Int J. Hyperthermia 23, 513–527 (2007). [PubMed: 17952765]
145. Yatvin MB, Weinstein JN, Dennis WH & Blumenthal R Design of liposomes for enhanced local release of drugs by hyperthermia. Science 202, 1290–1293 (1978). [PubMed: 364652] This study is the first to suggest that a thermal trigger could enhance drug delivery from liposomes constructed of lipids that undergo a temperature-dependent phase transition.
146. Gaber MH et al. Thermosensitive liposomes: extravasation and release of contents in tumor microvascular networks. Int. J. Radiat. Oncol. Biol. Phys 36, 1177–1187 (1996). [PubMed: 8985041]
147. Yarmolenko PS et al. Comparative effects of thermosensitive doxorubicin-containing liposomes and hyperthermia in human and murine tumours. Int. J. Hyperthermia 26, 485–498 (2010). [PubMed: 20597627]
148. Lokerse WJM et al. In depth study on thermosensitive liposomes: optimizing formulations for tumor specific therapy and *in vitro* to *in vivo* relations. Biomaterials 82, 138–150 (2016). [PubMed: 26761778]
149. Lu T, Lokerse WJM, Seynhaeve ALB, Koning GA & ten Hagen TLM Formulation and optimization of idarubicin thermosensitive liposomes provides ultrafast triggered release at mild

hyperthermia and improves tumor response. J. Control. Release 220, 425–437 (2015). [PubMed: 26541464]

150. Lindner LH et al. Dual role of hexadecylphosphocholine (miltefosine) in thermosensitive liposomes: active ingredient and mediator of drug release. J. Control. Release 125, 112–120 (2008). [PubMed: 18022271]
151. Needham D, Anyarambhatla G, Kong G & Dewhirst MW A new temperature-sensitive liposome for use with mild hyperthermia: characterization and testing in a human tumor xenograft model. Cancer Res 60, 1197–1201 (2000). [PubMed: 10728674]
152. Zagair TM. et al. Two phase I dose-escalation/pharmacokinetics studies of low temperature liposomal doxorubicin (LTLD) and mild local hyperthermia in heavily pretreated patients with local regionally recurrent breast cancer. Int. J. Hyperthermia 30, 285–294 (2014). [PubMed: 25144817]
153. Poon RTP & Borys N Lyso-thermosensitive liposomal doxorubicin: an adjuvant to increase the cure rate of radiofrequency ablation in liver cancer. Future Oncol 7, 937–945 (2011). [PubMed: 21823888]
154. US National Library of Medicine. ClinicalTrials.gov https://clinicaltrials.gov/ct2/show/NCT02112656 (2017).
155. US National Library of Medicine. ClinicalTrials.gov https://clinicaltrials.gov/ct2/show/NCT02181075 (2017).
156. Dou YN et al. Heat-activated thermosensitive liposomal cisplatin (HTLC) results in effective growth delay of cervical carcinoma in mice. J. Control. Release 178, 69–78(2014). [PubMed: 24440663]
157. Kakinuma K et al. Drug delivery to the brain using thermosensitive liposome and local hyperthermia. Int. J. Hyperthermia 12, 157–165 (1996). [PubMed: 8676003]
158. Weinstein JN, Magin RL, Yatvin MB & Zaharko DS Liposomes and local hyperthermia — selective delivery of methotrexate to heated tumors. Science 204, 188–191 (1979). [PubMed: 432641]
159. Chelvi TP, Jain SK & Ralhan R Hyperthermia-mediated targeted delivery of thermosensitive liposome-encapsulated melphalan in murine tumors. Oncol. Res 7, 393–398 (1995). [PubMed: 8747602]
160. Ponce AM et al. Magnetic resonance imaging of temperature-sensitive liposome release: drug dose painting and antitumor effects. J. Natl Cancer Inst 99, 53–63 (2007). [PubMed: 17202113]
161. Paoli EE et al. An optical and microPET assessment of thermally-sensitive liposome biodistribution in the Met-1 tumor model: importance of formulation. J. Control. Release 143, 13–22 (2010). [PubMed: 20006659]
162. Viglianti BL et al. *In vivo* monitoring of tissue pharmacokinetics of liposome/drug using MRI: illustration of targeted delivery. Magn. Reson. Med 51, 1153–1162 (2004). [PubMed: 15170835]
163. Grull H & Langereis S Hyperthermia-triggered drug delivery from temperature-sensitive liposomes using MRI-guided high intensity focused ultrasound. J. Control. Release 1 61,317–327 (2012).
164. Peller M et al. Surrogate MRI markers for hyperthermia-induced release of doxorubicin from thermosensitive liposomes in tumors. J. Control. Release 237, 138–146(2016). [PubMed: 27364227]
165. Ranjan A et al. Image-guided drug delivery with magnetic resonance guided high intensity focused ultrasound and temperature sensitive liposomes in a rabbit Vx2 tumor model. J. Control. Release 158, 487–494 (2012). [PubMed: 22210162]
166. Perez HL et al. Antibody-drug conjugates: current status and future directions. DrugDiscov. Today 19, 869–881 (2014).
167. Agarwal P & Bertozzi CR Site-specific antibody-drug conjugates: the nexus of bioorthogonal chemistry, protein engineering, and drug development. Bioconjugate Chem 26, 176–192 (2015).
168. Vasalou C, Helmlinger G & Gomes B A mechanistic tumor penetration model to guide antibody drug conjugate design. PLoS ONE 10, e0118977 (2015). [PubMed: 25786126]

169. Erickson HK et al. Antibody-maytansinoid conjugates are activated in targeted cancer cells by lysosomal degradation and linker-dependent intracellular processing. Cancer Res 66, 4426–4433 (2006). [PubMed: 16618769]

170. Maass KF, Kulkarni C, Betts AM & Wittrup KD Determination of cellular processing rates for a trastuzumab-maytansinoid antibody-drug conjugate (ADC) highlights key parameters for ADC design. AAPSJ. 18, 635–646 (2016). [PubMed: 26912181]

171. Diamantis N & Banerji U Antibody-drug conjugates — an emerging class of cancer treatment. Br: J. Cancer 114,362–367 (2016). [PubMed: 26742008]

172. Rich LJ et al. Enhanced tumour perfusion following treatment with water-filtered IR-A radiation to the thorax in a patient with head and neck cancer. Int. J. Hyperthermia 32, 539–542 (2016). [PubMed: 27150820]

173. Aziz SA et al. Vascularity of primary and metastatic renal cell carcinoma specimens. J. Transl Med 11,15 (2013). [PubMed: 23316728]

174. Liu JQ et al. PDGF-D improves drug delivery and efficacy via vascular normalization, but promotes lymphatic metastasis by activating CXCR4 in breast cancer. Clin. Cancer Res 17, 3638–3648 (2011). [PubMed: 21459800]

175. Shen G et al. SKLB1002, a novel inhibitor of VEGF receptor 2 signaling, induces vascular normalization to improve systemically administered chemotherapy efficacy. Neoplasma 59, 486–493 (2012). [PubMed: 22668017]

176. Viglianti BL et al. Systemic anti-tumour effects of local thermally sensitive liposome therapy. Int. J. Hyperthermia 30, 385–392 (2014). [PubMed: 25164143]

177. Wu J, Gong GH, Cui Y & Li RJ Intratumor partitioning and texture analysis of dynamic contrast-enhanced (DCE)-MRI identifies relevant tumor subregions to predict pathological response of breast cancer to neoadjuvant chemotherapy. J. Magn. Reson. Imag 76, 1107–1115 (2016).

178. Pascal J et al. Mechanistic patient-specific predictive correlation of tumor drug response with microenvironment and perfusion measurements. Proc. Natl Acad. Sci. USA 110, 14266–14271 (2013). [PubMed: 23940372]

179. Koay EJ et al. Transport properties of pancreatic cancer describe gemcitabine delivery and response. J. Clin. Invest 124, 1525–1536(2014). [PubMed: 24614108]

180. Wientjes MG Yeung BZ Lu Z, Wientjes MG & Au JL Predicting diffusive transport of cationic liposomes in 3-dimensional tumor spheroids. J. Control. Release 192, 10–18 (2014). [PubMed: 24995948]

181. Kerr DJ, Kerr AM, Freshney RI & Kaye SB Comparative intracellular uptake of adriamycin and 4′-deoxydoxorubicin by non-small cell lung tumor cells in culture and its relationship to cell survival. Biochem. Pharmacol 35, 2817–2823 (1986). [PubMed: 3741470]

182. Dewhirst MW, Secomb TW, Ong ET, Hsu R & Gross JF Determination of local oxygen consumption rates in tumors. Cancer Res 54, 3333–3336 (1994). [PubMed: 8012945]

Box 1|

Relative roles of convective and diffusive transport: the Péclet number

Consider a region where the solute concentration c(x) varies as a function of position x. According to Fick's first law of diffusion, the diffusive flux in the x direction is given by – D(dc/dx), where D is diffusivity. The convective flux is given by *uc,* where u is convective fluid velocity. If *C* is a typical concentration in the region under consideration, *U* is a typical velocity, and *L* is a typical length scale, then the concentration gradient dc/dx is of order *C/L,* a typical diffusive flux is *DC/L,* and a typical convective flux is *UC*. The dimensionless Péclet number *(Pe)* is defined as follows:

$$Pe = \frac{\text{convective flux}}{\text{diffusive flux}} = \frac{UL}{D}$$

The graph illustrates the dependence of the *UL/D* of the *Pe* on fluid velocity *U* and diffusivity *D*. The assumed length scale *L* = 100μm represents a typical spacing between microvessels. The right-hand scale indicates the relative molecular mass (M_r) corresponding to the diffusivity values according to the correlation of Swabb *etal.*[2]. Typical velocity ranges for interstitial fluid and for blood are indicated at the top. Note that the assumed diffusivity value for nanoparticles is based on results for 135 nm liposomes[180], and in this case, the M_r scale is therefore not applicable.

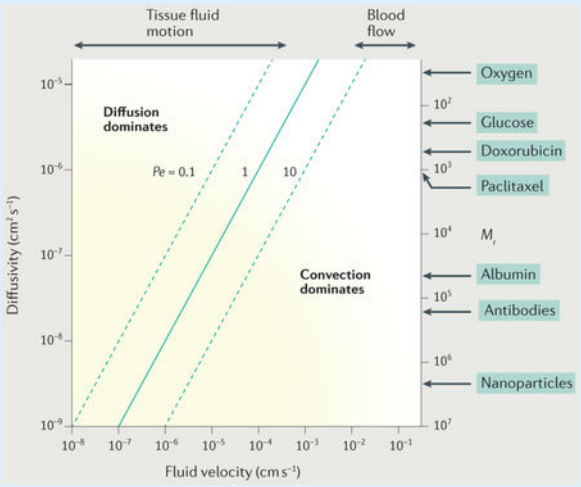

Box 2|

Estimation of solute penetration distance

Penetration distance can be estimated by considering steady-state transport in one spatial dimension, where c(x) is concentration as a function of distance x, $c(0) = c_0$ is the source concentration, x is distance from the source, and $c \to 0$ as $x \to \infty$. If the uptake kinetics are first order, that is, the uptake rate is $k_u c$, then for diffusion-dominated transport

$$c = c_0 \exp\left(-x / d_p\right), \text{where } d_p = \left(D / k_u\right)^{1/2} \quad (1)$$

Here, D is the diffusivity and d_p is the characteristic penetration distance. For convection-dominated transport with first-order kinetics, equation 1 applies but with $d_p = u/k_u$, where u is the fluid velocity. In the case of Michaelis-Menten uptake kinetics, if the source concentration is much larger than the Michaelis constant, zeroth-order kinetics can be assumed with a constant uptake rate V_m. Then, for diffusion-dominated transport

$$c = c_0\left(1 - x / d_p\right)^2 \text{for } x \le d_p, \text{where } d_p = \left(2Dc_0 / V_m\right)^{1/2} \quad (2)$$

and for convection-dominated transport

$$c = c_0\left(1 - x / d_p\right) \text{for } x \le d_p, \text{where } d_p = uc_0 / V_m \quad (3)$$

with c = 0for x > d_p in both cases. For nonlinear uptake kinetics, the penetration distance is again proportional to D 1/2 for diffusion-dominated transport and to u for convection-dominated transport, but a more complicated analysis is needed to obtain specific estimates.

The low-relative-molecular-mass (M_r) drug doxorubicin has a high cellular uptake rate, which limits its penetration distance even though its diffusivity is relatively high. *In vitro* uptake data[181] for a 30 min exposure at 0.5 μg ml^{-1} imply $k_u \sim 0.013\ s^{-1}$, for an average cell volume of 1,000 μm^3 and a volume fraction of cells in tissue of 0.5. The diffusivity based on M_r2 is $D = 2 \times 10^{-6} cm^2 s^{-1}$. Equation 1 gives d_p = 123μm, implying decay to $c_0/2$ over a distance of 85 μm. In reality, the uptake kinetics of doxorubicin are strongly nonlinear[181], and so this is only a rough estimate. Equation 2 can be applied to estimate the diffusion distance of oxygen from blood vessels[36]. For a typical tumour vessel with a partial pressure of oxygen (p_{02})of 30mmHg[39], the concentration in tissue adjacent to the vessel is about 40 μM or 9×10^{-4} cm3 O_2per cm^3. For a diffusivity $D = 1.5 \times lO^{-5}$ cm2 s^{-1} and a consumption rate[182] $V_m = 2.5 \times 10^{-4} cm^3$ O_2 per cm^3 per s, the diffusion distance is about 100 μm.

Pharmacokinetics

The time-dependent variation of drug concentrations in various compartments of the body following administration of a drug; often understood to refer to concentration in the blood plasma.

Pharmacodynamics

The dependence of therapeutic effects on the level and time course of exposure to a drug; for cancer therapies, therapeutic effect is often described in terms of cell survival fraction or tumour growth inhibition.

Enhanced permeability and retention (EPR) effect

The increased permeability of tumour microvessels relative to normal tissue vasculature, particularly in lipid and macromolecular agents and nanoparticles, leading to increased accumulation of such agents in the extravascular space in tumours. Enlarged gaps between endothelial cells occur where there is active angiogenesis. The gaps permit accumulation of nanoparticles within the tissue.

Diffusivity

A physical parameter describing the rate of molecular diffusion of a solute in the presence of a concentration gradient; defined as the ratio of the diffusive flux to the spatial derivative of concentration.

Hydraulic conductivity

A parameter defined as the ratio of the average fluid flow through the blood vessel wall per unit area divided by the net transmural (occurring across the entire vessel well) pressure driving filtration.

Tumour cords

Cylindrical masses of tumour cells with a small blood vessel running centrally along their axes, appearing in pathological sections as structures with a central vessel and concentric ring of viable tumour cells. A typical radius of up to 100–150 μm corresponds to the maximal diffusion distance of oxygen in tissue. Beyond the oxygen diffusion distance, necrosis is often observed.

Hypoxic regions

Tumour subregions where the partial pressure of oxygen (p_{02}) in tissue is > 0 and < 10 mmHg.

First-pass metabolism

The reduction in the concentration of a drug in blood as a result of the initial metabolism of the drug in the liver before reaching the systemic circulatory system.

Vascular endothelial growth factor

(VEGF). A cytokine (small protein) that potently stimulates blood vessel growth and increases vascular permeability.

Tortuosity

Pertaining to a blood vessel; the presence of multiple bends and twists in the path of the vessel between its branch points as quantified by the ratio of the length of the vessel measured along its curved path to the straight-line distance between branch points. In tumours, this ratio tends to be greater than one, whereas in normal tissue, it is close to one.

Vascular shunts

A relatively short, high-flow pathway from the arterial to the venous circulation. Identifiable shunt vessels are referred to as ‘anatomical shunts’, whereas shunting Occurring because of abnormal network structure is referred to as ‘functional shunting’.

Vessel wall shear stress

The tangential force per unit area exerted on a solid boundary by a moving fluid such as blood.

Stokes-Einstein radius

With reference to a solute, the radius of a hard sphere that diffuses at the same rate as the solute.

Multicellular layer system

An experimental system in which tumour cells are allowed to proliferate on a semipermeable membrane until they reach a thickness of several cell layers. The membrane is placed between two reservoirs, and drugs or other solutes that are added to one reservoir pass to the other reservoir by diffusion across the multiple layers. Rates of diffusion and metabolism are estimated from the rates at which the concentrations vary in the reservoirs.

Interstitial fluid pressure (IFP).

The hydrostatic pressure of the fluid that permeates the spaces between cells in a tissue; generally occurring as a result of fluid filtration from blood through the walls of blood vessels into the extravascular space.

K^{trans}

The rate constant describing the mass transfer between blood plasma and extravascular extracellular space per unit volume of tissue. This measurement is obtained using dynamic contrast-enhanced MRI.

Vascular rarefaction

A decrease in the total length of blood vessels per unit volume of tissue.

Dynamic contrast-enhanced MRI

(DCE-MRI]. A method used to quantify the change in signal intensity in tissue overtime after intravenous injection of an MRI contrast agent. The rates at which the contrast agent washes in and out of the tumour are used to estimate parameters related to perfusion and permeability of the microcirculation, including K^{trans}.

Texture analysis

A method used in image processing to assess the geometric arrangement of intensities within an image.

T1 relaxivity

In MRI, T1 relaxation time is the time constant for aligned spins to decay to baseline after an MR pulse. Relaxivity is a measurement of how a contrast agent influences the T1 relaxation time. With calibration, relaxivity can be used to measure concentration of the contrast agent in tissue.

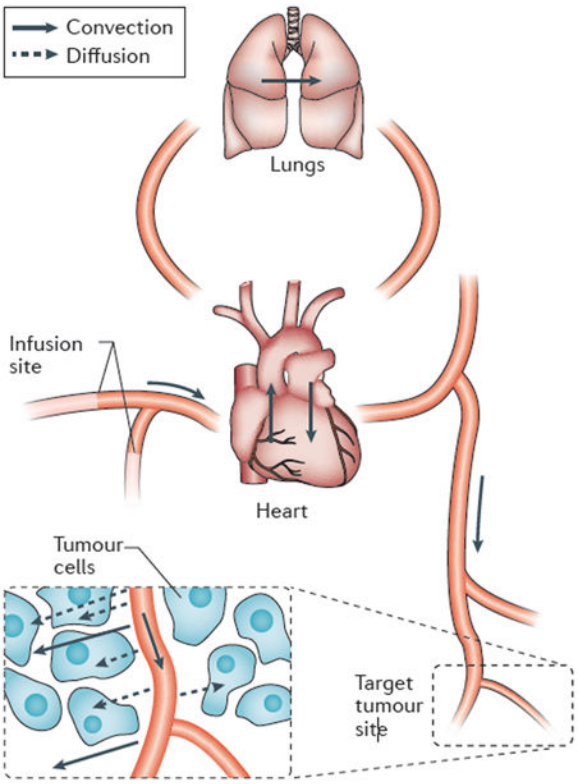

Figure 1 |. The pathway that drugs take from an intravenous infusion site to a solid tumour. Drug is transported by convection in the bloodstream through the systemic veins, the heart, the lungs and the systemic arteries to peripheral microvessels. Owing to rapid mixing of solutes in the blood, all parts of the circulatory system are exposed to the drug. Exchange between blood and tissue occurs primarily inthe microcirculation. Drug passes through microvessel walls and extravascular tissues to cancer cells by a combination of molecular diffusion and convection in interstitial fluid. Convective fluid motion in tissue is driven by fluid that filters through vessel walls. This fluid loss is balanced by resorption through other vessels and by the lymphatic system. For low-relative-molecular-mass drugs, diffusion is dominant over convection in the extravascular space.

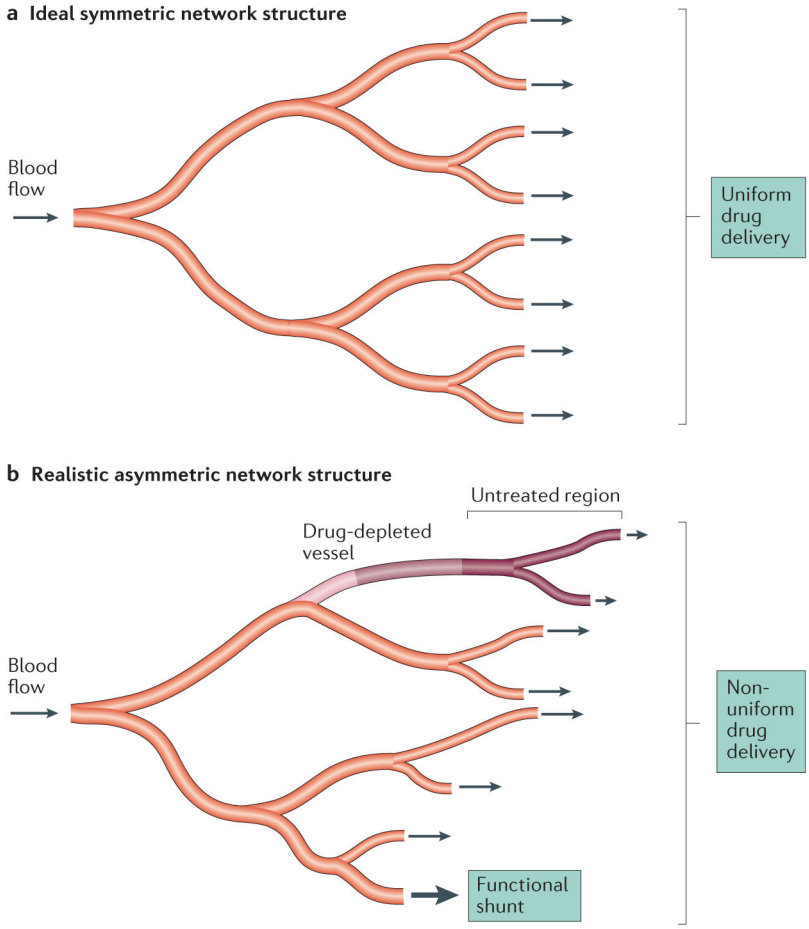

Figure 2 |. Limitations of drug transport within the microcirculation.

a | Microvascular networks are often depicted as having ideal symmetric branching structures so that drugs in the blood are uniformly distributed throughout the branches of the network, **b** | In reality, microvascular networks have highly asymmetric structures with extensive variation among branches in flow path lengths and blood flow rates. Some branches receive very low flow, and the drug may be depleted before the terminal branches are reached, such that some tissue regions are not treated. Conversely, short high-flow pathways may form functional shunts between the arterial and venous systems, greatly restricting exchange of solute between blood and tissue. This effect is accentuated in tumours relative to normal tissues.

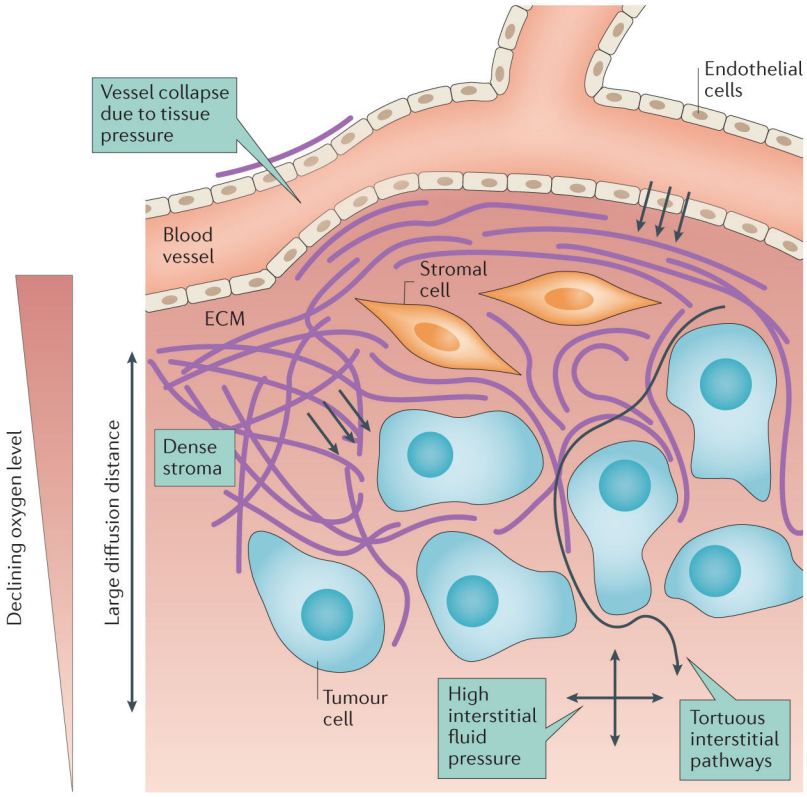

Figure 3 |. Limitations of drug transport in extravascular tissue.

A drug must pass several potential barriers in order to reach tumour cells. High tissue pressures may cause vessel collapse, restricting blood flow. The endothelial cells lining microvessels restrict extravasation of drug. Dense stroma, consisting of extracellular matrix (ECM) and cells such as fibroblasts, can be a physical barrier, particularly for large molecules and nanoparticles, and is a binding site for some drugs. The pathway for transport within tumours may be tortuous owing to stroma and parenchymal cells. Large transport distances may result in incomplete drug distribution. High interstitial fluid pressure (IFP) acting in all directions (denoted by the crossed arrows) may reduce fluid flow and restrict drug delivery by convection. Pink background shading represents the oxygen level decreasing with distance from the blood vessel.

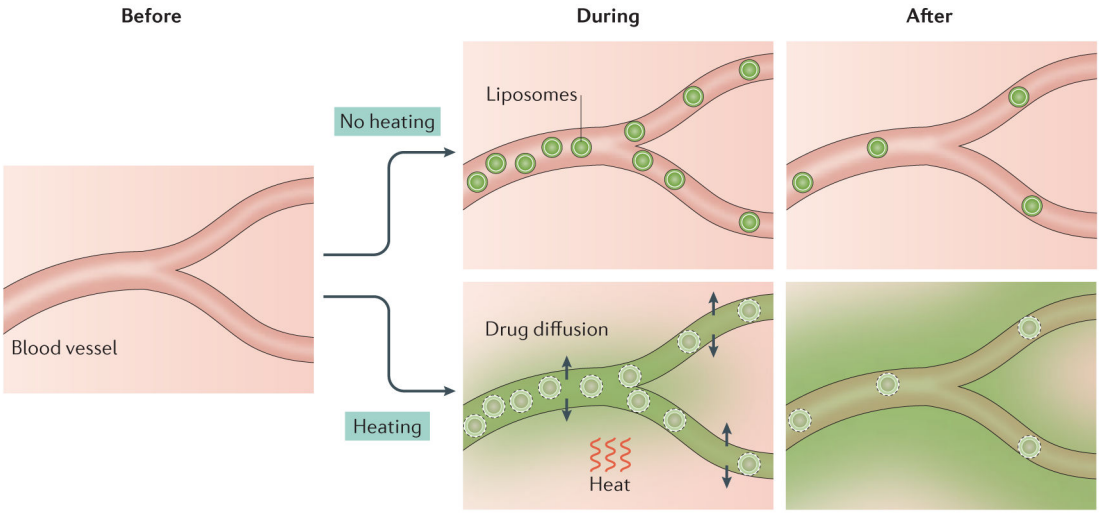

Figure 4 |. Principle of thermally triggered drug release from liposomes.
This illustration is based on experimental imaging of drug distribution[54]. Local application of heat during the delivery of liposomes causes pores to form in the lipid bilayer and thus release of drug, which diffuses into the tissue. With heating, penetration of liposomes through blood vessel walls into tissue is not required for drug delivery to tumour. Here, drug release occurs intravascularly. Green shading indicates the level of drug.

Table 1 |

Factors in drug delivery to solid tumours

Factor	Drug size and type		
	M_r <1000	M_r >1,000	Nanoparticle
Drug characteristics			
Size and shape	+	+	+
Charge distribution	+	+	+
Surface coating	−	−	+
Lipid solubility	+	+	+
Acid–base characteristics	+	−	-
Physiological factors			
Pharmacokinetics	+	+	+
Vascular density	+	+	+
Arteriovenous shunting	+	+	+
Microvessel permeability	−	+	+
Microvessel pore size	−	−	+
Extent and density of ECM	+	+	+
IFP	−	+	+
Tissue pressure	+	+	+

+, important factor; -, not an important factor; ECM, extracellular matrix; IFP, interstitial fluid pressure; M_r, relative moiecuiar mass.